Digital Signal Processing 95 (2019) 102577

Contents lists available at ScienceDirect

Digital Signal Processing

www.elsevier.com/locate/dsp

Blind parameter estimation of turbo convolutional codes: Noisy and non-synchronized scenario

Swaminathan R [a,*], A.S. Madhukumar [b]

[a] Discipline of Electrical Engineering, Indian Institute of Technology Indore, Indore-453552, India
[b] School of Computer Science and Engineering, Nanyang Technological University, Singapore-639798, Singapore

ARTICLE INFO

Article history:
Available online 29 August 2019

Keywords:
Adaptive modulation and coding
Blind estimation
Non-cooperative systems
Reconfigurable receiver systems
Recursive systematic convolutional codes
And turbo convolutional codes

ABSTRACT

Blind estimation of forward error correction code parameters at the receiver plays a significant role in non-cooperative communication, adaptive modulation and coding systems, and reconfigurable receiver systems. Turbo convolutional codes, a parallel concatenation of multiple convolutional codes, are used in digital communication and storage systems to achieve low bit error rate. The present paper proposes innovative algorithms for the blind estimation of code parameters and reconstruction of turbo convolutional encoder over noisy scenario. The turbo convolutional code is designed using two component codes along with an interleaver. Recursive systematic convolutional codes are used as component codes. Any imperfection in synchronization of received data for the proposed code parameter estimation algorithm is compensated through a bit position adjustment parameter. The performance of the proposed algorithms in terms of parameter estimation accuracy is investigated for different modulation order, code rate, and constraint length values. It is observed that the performance improves with decrease in modulation order and constraint length values.

1. Introduction

Forward error correction (FEC) codes and interleavers improve the error performance of digital communication and storage systems by counteracting random and burst errors. Parameter estimation of an unknown FEC code from noisy codewords is related to cryptanalysis and is called the code parameter estimation problem in the literature. Here, an observer wants to decode the information bits from a noisy data stream, where the FEC code used for transmission is unknown. This scenario mainly arises in a non-cooperative context [1], [2], where erroneous binary sequence is acquired from an unknown communication system. Non-cooperative scenarios exist particularly in electronic warfare, military, spectrum surveillance, signals intelligence (SIGINT), and communications intelligence (COMINT) systems. Due to recent advancements in modern digital communication techniques, it is always a costly and tedious process to design separate receivers for every standards in use around the world. Thus, there is a need for an intelligent receiver system which adapts itself to any applications [3], [4]. Hence, reconfigurable radio systems are introduced. It is also essential to blindly estimate the code parameters of an ideal reconfigurable radio in order to adapt to the variations in the channel encoders for decoding the message symbols successfully.

The blind reconstruction of channel encoder is also useful in adaptive modulation and coding i.e. AMC-based systems. The modulation and FEC code parameters are usually communicated to the receiver through control channel in AMC systems. The blind recognition of type of modulation schemes and FEC code parameters will result in conserving the channel resources and improve the spectral efficiency of the AMC-based systems as mentioned in [5], [6], [7], and [8]. Recently, cumulants-based framework was proposed in [5] for automatic modulation classification. The wireless sensor networks (WSNs) also use AMC technique to choose different encoders. The blind reconstruction techniques will reduce the energy consumption of WSNs, as it is not essential to transmit the overhead information to the sensor nodes in order to indicate the changes in code parameters.

In literature, different algorithms were proposed for the blind estimation of FEC code parameters. Firstly, algorithms for code classification and code parameter estimation were given for non-erroneous (i.e. noiseless) scenario in [1]. The algorithms for the blind estimation of convolutional code parameters were proposed for noisy scenario in [3], [4], and [9]. In [10], the algebraic properties of the convolutional encoders, which are useful for blind recognition in cognitive radio systems, were investigated. The blind recognition algorithm to extract the parent code parameters from

* Corresponding author.
E-mail addresses: swamiramabadran@iiti.ac.in (R. Swaminathan), asmadhukumar@ntu.edu.sg (A.S. Madhukumar).

https://doi.org/10.1016/j.dsp.2019.102577
1051-2004/

noisy punctured convolutional coded data symbols was proposed in [11]. Recently, code classification algorithms were proposed in [12] to classify the incoming binary data symbols among block, convolutional coded, and uncoded data symbols. The proposed algorithms also estimate block interleaver parameters over noisy transmission environment. The algorithms for the blind estimation of codeword length of various non-binary error correcting codes were proposed in [13] for noisy environment. In [14], the blind estimation algorithm to extract the parameters of Reed-Solomon (RS) codes over erroneous channel conditions was reported. The proposed method is based on Barbier's dual code method [15]. Recently, algorithms for the blind estimation of RS code and block interleaver parameters were proposed in [16]. The blind reconstruction of true channel encoder within a candidate set for low-density parity-check (LDPC), RS, and convolutional codes based on the soft-decision outputs i.e. average log-likelihood ratio (LLR) of syndrome aposteriori probability was reported in [6], [7], and [8], respectively.

In [17] and [18], the blind reconstruction of turbo convolutional encoders was investigated using iterative expectation-maximization (EM) and least square methods, respectively. In both the methods, parallel concatenation of two recursive systematic convolutional (RSC) encoders with interleaver was considered. However, only the first RSC encoder was estimated without estimating the second one and interleaver. Moreover, the constraint length of the RSC encoder was also assumed to be known at the receiver in [17]. An efficient algorithm for recovering the permutation of the interleaver in turbo encoder was proposed in [19]. The problem of reconstruction of the turbo encoder system has also been addressed in [20] and a method to estimate turbo convolutional code (TCC) parameters was given. However, the proposed method estimates only total codeword length and code dimension of TCCs assuming two identical RSC encoders without estimating the parameters of individual constituent RSC encoders and interleavers. The algorithms for the parameter estimation of block interleaver were proposed in [2], [12], [15], [16], [21], and [22]. Similarly, the algorithms for the parameter estimation of convolutional interleaver were reported in [23], [24], and [25] considering linear block encoded, convolutional coded, and RS coded data symbols, respectively. Recently, novel algorithms were proposed to estimate the interleaver size in [2] and [26] by exploiting the linear dependence among the received noisy codewords. However, algorithms for the blind estimation of all the code and interleaver parameters of TCCs (without the knowledge of important code/interleaver parameters) have not been proposed in any of the existing works. In this context, the major motivations and contributions of the present research are as follows:

1.1. Motivations

The main motivations are given as follows:

- It is always mandatory to reconstruct the channel encoder at the receiver from noisy data stream in a non-cooperative system.
- To design a reconfigurable channel decoder that is compatible to any communication standards by blindly estimating the FEC code parameters.
- Previously proposed algorithms for TCCs in [17] and [18] were restricted only to the blind reconstruction of first RSC encoder without reconstructing the second RSC encoder and interleaver. Moreover, critical parameters like constraint length was assumed to be known at the receiver in [17].
- In [19], only permutation of the interleaver considered in the turbo encoder was identified without estimating the RSC encoder parameters.
- The proposed algorithm in [20] recognized the total codeword length and code dimension of TCCs without estimating the parameters of individual constituent RSC encoders and interleavers.
- In addition, the proposed algorithms or methods in [17–20] were limited only to synchronized environment.
- In a nutshell, two non-identical RSC encoder parameters along with interleaver parameters and bit position adjustment parameter, which are essential to reconstruct the turbo encoder and achieve frame synchronization, were not recognized in any of the existing works to the best of our knowledge.

1.2. Contributions

The main contributions are as follows:

- Innovative algorithms for the blind reconstruction of turbo encoder considering two parallel concatenated RSC encoders and a matrix-based block interleaver are given for non-erroneous (noiseless) and erroneous (noisy) scenarios. The estimated parameters are grouped as follows: (1) codeword length and code dimension of TCC, (2) individual codeword lengths, code dimensions, and constraint lengths of RSC encoders, (3) rank deficiency difference, number of rows, and number of columns of block interleaver matrix.
- Apart from the code parameters, the bit position adjustment parameter to achieve frame synchronization is also estimated using the proposed algorithms.
- The performance of the proposed algorithms in terms of parameter estimation accuracy is extensively analyzed for different $M-$ary quadrature amplitude modulation ($M-$QAM) schemes and code parameters.

1.3. Comparison with our prior works

In [12], the code classification algorithms (with and without interleaver) were proposed to classify the incoming coded symbols among block and convolutional codes. Moreover, important code and block interleaver parameters were also identified for synchronized and noisy scenario. Recently in [16], novel algorithms were proposed to jointly estimate the code and interleaver parameters of RS codes and block interleaver, respectively, over non-synchronized and noisy environment. In [21], algorithms were proposed to estimate the parameters of block and convolutional interleavers from convolutional coded data in the presence of bit errors. In our current work, we have proposed innovative algorithms for the blind reconstruction of turbo encoder considering two parallel concatenated RSC encoders and a matrix-based block interleaver along with achieving frame synchronization. The algorithms in [16] are applicable to finite field, since RS code is a non-binary code. The algorithms proposed in [21] can only estimate interleaver parameters but not convolutional code parameters. The parameter estimation steps of the current work (refer to Fig. 4) are completely different compared to [12], [16] and [21].

Though the rank-deficiency-based approach is applied in our current work to estimate RSC encoder and interleaver parameters similar to [12], [16] and [21], the proposed algorithms are not a trivial combination of our algorithms proposed in prior works. Precisely, Algorithms 1 and 2, which are proposed to identify the total codeword length, code dimension of TCC, and rank deficiency difference parameter of interleaver, are the modified versions of the algorithms proposed in our prior work [12]. However, the vital parameters such as code parameters of individual RSC encoders, interleaver parameters, and bit adjustment parameter to achieve synchronization are identified using innovative algorithms (Algorithms 3 and 4), which are proposed exclusively in the current

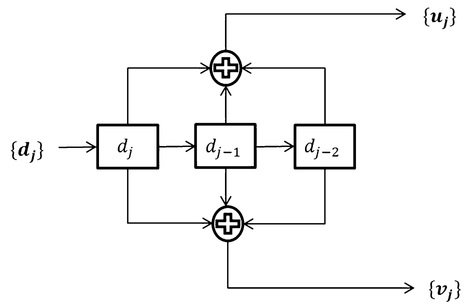

Fig. 1. Non-systematic convolutional encoder.

work. Further, the rank equations (4) to (8) obtained using Algorithms 1 and 2 in the current work are entirely different from the rank equations obtained in [12], [16], and [21]. In particular, the non-contiguous deficient rank values are not observed in our prior works. Here, identification of non-contiguous deficient rank values, which is given by (8), plays a pivotal role in estimating interleaver parameters. The case studies explaining the rank equations (Appendix A and B) are also different from our previous works. Thus, the novelty of the proposed algorithms compared to the existing algorithms lies in the following aspects: (1) Blind reconstruction of two non-identical RSC encoders and interleaver of TCCs; (2) Blind estimation of bit adjustment parameter to achieve frame synchronization. To the best of our knowledge, none of the existing methods have recognized all the parameters of turbo convolutional encoder and achieved frame synchronization over erroneous channel conditions.

1.4. Organization of the manuscript

The manuscript is organized as follows. In Section 2, an introduction about TCC and block interleaver is given and in Section 3, the parameter estimation process has been explained using generic block diagram. The algorithms for the blind reconstruction of turbo convolutional encoder over noiseless and noisy scenarios along with detailed discussions are given in Section 4 and 5, respectively. In Section 6, the simulation results and discussions are given for various test cases along with the performance of the proposed algorithms. Finally, concluding remarks are given in Section 7.

2. Turbo codes and Block interleavers

In this section, we will first explain the difference between non-systematic and recursive systematic convolutional encoders. After that turbo convolutional encoders are formed by the parallel concatenation of RSC encoders.

In case of non-systematic convolutional encoders with rate $r = 1/n$, constraint length K, and memory order $m = K - 1$, the output codeword at time instant j is the bit pair (u_j, v_j) corresponding to the input bit d_j. The expressions for bit pair u_j and v_j are, respectively, given by

$$u_j = \sum_{i=0}^{m} g_{1i} d_{j-i} \text{ modulo} - 2\,, \;\; g_{1i} = 0, 1 \tag{1}$$

and

$$v_j = \sum_{i=0}^{m} g_{2i} d_{j-i} \text{ modulo} - 2\,, \;\; g_{2i} = 0, 1 \tag{2}$$

Note that $g_1 = \{g_{1i}\}$ and $g_2 = \{g_{2i}\}$ are the code generators and they are given by $g_1 = \{1\ 1\ 1\}$ and $g_2 = \{1\ 0\ 1\}$ for the rate 1/2 non-systematic convolutional (NSC) encoder with K=3 as shown in Fig. 1. It is also a well known fact the error performance of NSC codes is better than RSC codes for high signal-to-noise ratio (SNR) values. The NSC encoder can also be visualized as a finite impulse response (FIR) linear system. On the contrary, a class of infinite impulse response (IIR) system has been proposed as a building block for TCCs and they are also called as RSC codes. For high code rate values, the error performance of RSC codes is better than NSC codes irrespective of the SNR values. A RSC encoder is obtained from NSC encoder with the help of a feedback loop and by making one of the outputs (u_j or v_j) equal to input d_j. In Fig. 2, an example for rate 1/2 RSC encoder is shown assuming $u_j = d_j$ and $K = 3$ and a_j is calculated recursively as follows

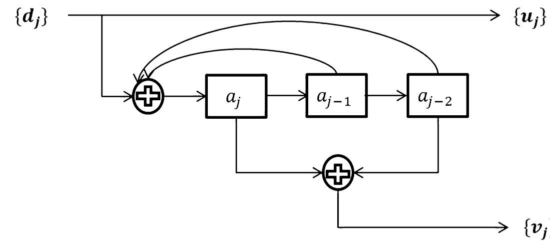

Fig. 2. Recursive systematic convolutional encoder.

$$a_j = d_j + \sum_{i=1}^{m=2} g_{1i} a_{j-i} \text{ modulo} - 2\,. \tag{3}$$

Turbo convolutional encoder is a parallel concatenation of RSC encoders with interleavers in parallel. The parallel concatenated convolutional coding along with iterative decoding principles has led to their absorption in a wide variety of applications some of which include deep space communications, 3G and 4G mobile telephony standards, and digital video broadcasting (DVB) [27]. This is because, TCCs have exceptionally good performance as low as 10^{-5} at SNR within 1 dB of Shannon limit. Hence, the error performance of TCCs is better than the previously proposed FEC codes by several decibels with comparable decoding complexity. A block diagram of rate 1/3 turbo convolutional encoder comprising of two RSC encoders and an interleaver is shown in Fig. 3. Here, the information sequence is assumed to be a block of L information bits and it is represented as $\mathbf{d_j} = (d_0, d_1, \cdot, \cdot, \cdot, d_{L-1})$. Since the encoder is systematic, the first transmitted sequence is nothing but the information sequence and it is given by $\mathbf{v_j^{(0)}} = \mathbf{d_j} = (v_0^{(0)}, v_1^{(0)}, \cdot, \cdot, \cdot, v_{L-1}^{(0)})$. The second transmitted sequence is the parity sequence generated from the first encoder and the same is given by $\mathbf{v_j^{(1)}} = (v_0^{(1)}, v_1^{(1)}, \cdot, \cdot, \cdot, v_{L-1}^{(1)})$. The interleaver permutes the information sequence depending upon the type of interleaver and the permuted sequence $\mathbf{d'}$ is sent as the modified information sequence for the second encoder. From the figure, it is observed that the third transmitted sequence is the parity sequence generated from the second RSC encoder and it is given by $\mathbf{v_j^{(2)}} = (v_0^{(2)}, v_1^{(2)}, \cdot, \cdot, \cdot, v_{L-1}^{(2)})$. Now the final transmitted sequence of rate $r = 1/3$ turbo convolutional encoder is given by $\mathbf{v} = (v_0^{(0)}, v_0^{(1)}, v_0^{(2)}, v_1^{(0)}, v_1^{(1)}, v_1^{(2)}, \cdot, \cdot, \cdot, v_{L-1}^{(0)}, v_{L-1}^{(1)}, v_{L-1}^{(2)})$.

For generating the permuted sequence as described above, a matrix-based block interleaver is considered in our work and its operation is given as follows: The incoming data stream is divided into multiple blocks each of size equal to size of interleaver matrix or interleaver period β, where $\beta = N_r \times N_c$, N_r and N_c denote the number of rows and columns of the matrix, respectively. The interleaver stores the data symbols row-wise in the matrix and interleaves column-wise. It is to be noted that the application of matrix-based block interleaver in turbo codes provides better performance compared to random interleavers for short block

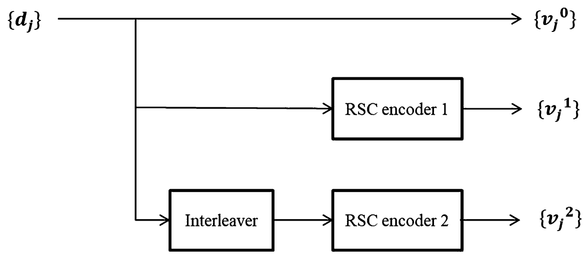

Fig. 3. Basic Turbo encoding structure.

lengths [27]. In addition, short block lengths are mandatory for next-generation communication systems to keep the delay requirements within the acceptable limits.

3. Code parameter estimation process

The block diagram of the parameter estimation process of TCC is given in Fig. 4. At the transmitting end, the turbo convolutional coded binary data symbols are modulated using appropriate modulation schemes for transmission. At the receiving end, the blind reconstruction process is carried out in three steps. The codeword length and code dimension of TCC along with rank deficiency difference parameter will be identified in the first step. The rank deficiency difference is an intermediate parameter which is to be estimated in order to estimate the individual block interleaver parameters. After that the individual block interleaver parameters i.e. number of rows N_r and number of columns N_c of block interleaver matrix will be recognized.

At the receiver, the beginning of the received codewords should be recognized before decoding so that the decoder functions properly. This is called frame synchronization. Here, we assume that the incoming turbo convolutional coded sequence at the receiver is not synchronized and it is essential to recognize the starting position of the received codeword. Thus, we adopt blind frame synchronization technique to estimate bit adjustment parameter in order to achieve synchronization apart from estimating code and interleaver parameters. If the received codewords are assumed to be synchronized, then frame synchronization is not essential at the receiver. Finally, the code dimensions, codeword lengths, and constraint length values of individual RSC encoders will be estimated. Note that the generator polynomials of the respective RSC encoders should be identified to complete the parameter estimation process. We have not assumed that the generator polynomials are known apriori. However, in this manuscript, we will not discuss about the estimation of generator polynomials, as several algorithms were proposed in [3], [4], and [10] to estimate the same. We assume that the receiver frames are not synchronized by introducing bit offset at the receiver. The receiver only knows that the incoming data is turbo convolutional encoded using two RSC encoders and block interleaver.

4. Parameter estimation of TCC: non-erroneous scenario

The notations, which are common to all proposed algorithms, are given as follows:
Notations: Let b and a indicate the number of columns and rows of data matrix S, respectively. Let F denotes the column echelon form of S. Let N_r and N_c denote the number of rows and columns of block interleaver matrix, respectively. The rank deficiency difference is denoted by Δ. The parameters m_i, n_i, k_i, and K_i denote memory order, codeword length, code dimension, and constraint length of RSC encoders, respectively. Note that the subscript $i=1$ and 2 indicate first and second RSC encoders, respectively. Let n and k denote the codeword length and code dimension of TCC, respectively. For simplicity, we assume $k_1=k_2=k$ and the codeword length of TCC is given by n_1+n_2-k.

The parameter estimation of codeword length and code dimension of TCC along with rank deficiency difference parameter over non-erroneous scenario is explained using Algorithm 1. The incoming turbo convolutional encoded binary symbols are reshaped into a matrix S of size $a\times b$, where $b\in[b_{\min}, b_{\max}]$. Since S contains binary data symbols, the matrix S is called data matrix. The rank and rank ratio of S are calculated using Gauss elimination process. It is a known fact that the Gauss elimination process removes all the dependent rows or columns of a given matrix and convert it into a row or column echelon form and the number of linearly independent rows/columns gives the rank of a matrix. Otherwise, the number of non-zero rows/columns of row/column echelon form gives the rank of a matrix. Rank ratio indicates the ratio of the rank of a matrix to the number of columns. If the rank ratio is equal to unity or if rank of S is equal to $\min(a,b)$ or if all the rows and columns of S are linearly independent, then S is called full rank matrix. However, if the rank of S is less than $\min(a,b)$ or rank ratio is less than unity or if there is at least one dependent column/row, then S is called deficient rank matrix. The difference between successive number of columns with rank deficiency and corresponding deficient rank values are stored in row vectors A and B, respectively. The codeword length and code dimension of the turbo encoder are obtained by recognizing the most frequent value in the row vectors A and B, respectively, as given in steps 6 and 8 of Algorithm 1. The estimated values of n and k are denoted by n^{est} and k^{est}, respectively. Similarly, the difference between successive number of columns with non-contiguous deficient rank values, which is denoted by $\Delta'=n\cdot\beta$, is also stored in another row vector C. The rank deficiency difference parameter Δ is estimated from the most frequent value in the row vector C as shown in step 11 of Algorithm 1. Note that the rank deficiency difference is an intermediate parameter necessary to identify N_r and N_c. The estimated value of Δ is denoted by Δ^{est}.

The bounds for the rank values of TCC with block interleaver under synchronized scenario are given as follows: Assuming $k_1=k_2=k$, $n_1\geq 2$ and $n_2-k_2=1$, if b is a multiple of n (i.e. $b=\alpha'\cdot n$),

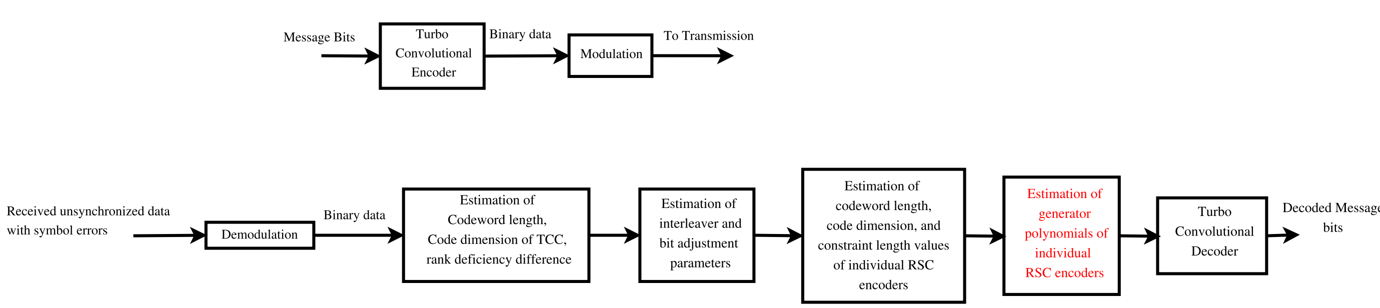

Fig. 4. Block diagram for parameter estimation of TCCs.

Algorithm 1: Estimation of code word length, code dimension, and rank deficiency difference parameters (Non-erroneous conditions).

Notations: Let $\rho(S)$ and $p(S)$ denote the rank and rank ratio of S, respectively;
Assumptions: $a \geq b$ and $b \in [b_{\min}, b_{\max}]$;
Input: Turbo convolutional coded binary data symbols;
Output: n^{est}, k^{est}, and Δ^{est};
1:**for** $b = b_{min} : b_{max}$ **do**
  2: Reshape the incoming turbo encoded data symbols into a matrix S of size $a \times b$;
  3: Convert S into F using Gauss elimination process;
  4: Evaluate $\rho(S)$ from the number of non-zero columns in F and $p(S)$ is given by $p(S) = \rho(S)/b$;
end
5: Observe the difference between successive number of columns with deficient rank values and accumulate the values in a row vector A;
6: The codeword length n^{est} is estimated from the most frequent value in the row vector A;
7: Observe the difference between successive rank values corresponding to the rank deficient columns and accumulate the values in a row vector B;
8: The code dimension k^{est} is estimated from the most frequent value in the row vector B, which is denoted by $\hat{\gamma}'$, as follows: $k^{\text{est}} = \hat{\gamma}' - 1$;
9: Observe the difference between successive number of columns with non-contiguous deficient rank values and accumulate the same in row vector C;
10: Observe the most frequent value in the set C and is denoted by Δ';
11: The rank deficiency difference Δ for block interleaver is estimated as $\Delta^{\text{est}} = \frac{\Delta' . k^{\text{est}}}{n^{\text{est}}}$;

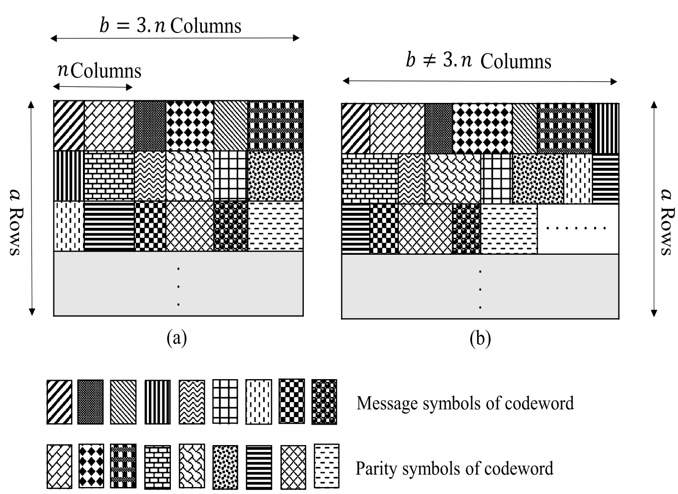

Fig. 5. Structure of data matrix for the case when (a) $b = 3 \cdot n$ and (b) $b \neq 3 \cdot n$.

then rank of S for the case when b is a not a multiple of Δ' (i.e. $b \neq \alpha \cdot \Delta'$) is given by

$$\rho(S) \leq \alpha' \cdot (k+1) + m_1 < b\,, \tag{4}$$

where α and α' are positive integers and if $b \neq \alpha' \cdot n$, then rank of S is given by

$$\rho(S) \leq b\,. \tag{5}$$

The reasons for deficient rank, which is given by (4) and full rank (with high probability), which is given by (5), are given as follows: Due to inherent property of convolutional codes, n_1 coded output data bits depend on k present and m_1 previous input uncoded data bits as mentioned in [3] and [12]. Hence, $\alpha' \cdot n_1$ output bits depend on $\alpha' \cdot k$ present and m_1 previous bits. As depicted in Fig. 5(a), it is observed that the message and parity bits of α' codewords in all the rows will be aligned properly in the same column only for the case when b is a multiple of n i.e. $b = \alpha' \cdot n$. Note that $\alpha' = 3$ in Fig. 5. If the alignment is proper across all the rows, the linear relation will be satisfied in all the rows, which will eventually lead to the existence of linear relations between columns in S. After converting S into F through Gauss elimination process, there will be only $\alpha' \cdot k + m_1$ non-zero or independent columns out of b columns in the case of first RSC encoder. Since it has been assumed that $n_2 - k_2 = 1$, each turbo convolutional codeword contains only one parity bit from second RSC encoder without message bits due to puncturing. Thus, α' parity bits from second RSC encoder without message bits will result in another α' independent columns due to non-existence of linear relations between columns. In a nutshell, $\alpha' \cdot k + m_1 + \alpha'$ independent columns out of b columns will be observed and the number of independent columns gives the rank of the matrix as given by (4). Moreover, if b is not a multiple of n, then the message and parity bits will not be aligned properly across all the rows in the same column as shown in Fig. 5(b). Hence, linear relations will not exist between the columns, which might eventually lead to full rank with high probability as given by (5). It is to be noted that the probability of obtaining rank values greater than or equal to $l-1$ for a random binary square matrix [26] of size $l \times l$ is more than 0.85. The rank equations (4) and (5) are also explained in Appendix A using case study 1.

Assuming $n_1 \geq 2$ and $n_2 - k_2 > 1$, if $b = \alpha' \cdot n$, then rank of S for the case when $b \neq \alpha \cdot \Delta'$ is given by

$$\rho(S) \leq \alpha' \cdot (k_1 + k_2) + m_1 + m_2 < b \tag{6}$$

Assuming $k_1 = k_2 = k$, $\rho(S) \leq \alpha' \cdot 2 \cdot k + m_1 + m_2$. If $b \neq \alpha' \cdot n$, then rank of S is given by

$$\rho(S) \leq b\,. \tag{7}$$

For the case when $n_2 - k_2 > 1$, each turbo convolutional codeword contains more than one parity bit from second RSC encoder without message bits. Since $\alpha' \cdot (n_2 - k_2)$ parity bits are aligned properly in the same column, they will act as coded bits unlike the case when $n_2 - k_2 = 1$. Therefore, $\alpha' \cdot (n_2 - k_2)$ columns due to second RSC encoder in S will result in $\alpha' \cdot k_2 + m_2$ independent columns in addition to $\alpha' \cdot k_1 + m_1$ columns due to first RSC encoder. To sum up, $\alpha' \cdot (k_1 + k_2) + m_1 + m_2$ independent columns will be observed out of b columns in total after Gauss elimination process as given by (6). As already mentioned, for the case when b is not a multiple of n, full rank will be obtained with high probability as given by (7) due to misalignment of data and parity bits. The rank equations (6) and (7) are also explained in Appendix B using case study 2.

Assuming $k_1 = k_2 = k$, if $b = \alpha \cdot \Delta'$, where $\Delta' = \beta \cdot n$, then rank of S is given by

$$\rho(S) \leq \beta \cdot \alpha \cdot k + m_1 + m_2 < b\,. \tag{8}$$

When b is a multiple of Δ', where $\Delta' = \beta \cdot n$, block of $\beta \cdot n$ coded bits from two RSC encoders will be viewed as the bits generated from single convolutional encoder whose memory is equal to $m_1 + m_2$. This is because, the parity bits from the second RSC encoder can be represented as a linear combination of systematic message bits only at multiples of $\beta \cdot n$. However, for other values of b, only few or no parity bits generated from the second RSC encoder can be represented as a linear combination of message bits due to incomplete interleaving of message bits. Hence, for the case when $b = \alpha \cdot \beta \cdot n$, the parity and message bits of $\beta \cdot \alpha$ codewords will be aligned properly in the same column across all the rows. After converting the data matrix into column echelon form, at most $\beta \cdot \alpha \cdot k + m_1 + m_2$ non-zero columns out of b columns will be observed as given by (8). Since the deficient rank values obtained from (8) follow different trend compared to (4) and (6), they are called non-contiguous deficient rank values. The rank equation (8) is also explained in Appendix A using case study 1.

Let $b = \alpha' \cdot n$ and $b' = (\alpha' + 1) \cdot n$ indicate the number of columns corresponding to two rank deficient matrices and their difference is given by

$$b' - b = (\alpha' + 1) \cdot n - \alpha' \cdot n = n \tag{9}$$

Similarly, $b = \alpha \cdot \Delta'$ and $b' = (\alpha + 1) \cdot \Delta'$ denote the number of columns corresponding to two non-contiguous rank deficient matrices and the corresponding difference is given by

$$b' - b = (\alpha + 1) \cdot \Delta' - \alpha \cdot \Delta' = \Delta' \tag{10}$$

Hence, it can be observed that the codeword length n of TCC and Δ', which is an intermediate parameter to estimate rank deficiency difference Δ, can be identified from (9) and (10), respectively.

5. Parameter estimation of TCC: erroneous scenario

The parameter estimation of codeword length, code dimension of TCC, and rank deficiency difference over erroneous channel conditions is explained using Algorithm 2. The dependent columns in S will be eliminated using Gauss elimination process and the deficient rank value is calculated from the number of non-zero columns in the column echelon form for non-erroneous scenario. However, the deficient rank values calculated using Algorithm 1 for noisy scenario will not be precise. This is mainly due to the presence of transmission errors or white noise, which will increase the linear independence among rows/columns of a deficient rank matrix. Hence, full rank with high probability will be obtained irrespective of the number of columns b [16]. It is noticed that the dependent columns in the column echelon form of rank deficient data matrix will have more number of zero elements compared to independent columns over erroneous channel conditions. Hence, the dependent or independent columns can be classified based on the ratio of zero elements in the particular column of F over N iterations [12] and accordingly, Algorithm 1 is modified for erroneous or noisy scenario. The ratio of zero elements, which is denoted by $\omega_j(c)$, is defined as the ratio of number of zeros in a particular column to the total number of rows. After classifying the dependent and independent columns based on the ratio of zero elements over N iterations, rank or rank ratio values are calculated from the number of independent columns as shown in step 10 of Algorithm 2. From the rank and rank ratio values, TCC parameters are estimated similar to Algorithm 1.

In Algorithm 3, the steps are given for the estimation of matrix-based block interleaver parameters N_r and N_c, synchronization parameter ϕ, and codeword lengths of individual RSC encoder n_1 and n_2 over erroneous channel conditions. The parameters are estimated based on TCC parameters n^{est}, k^{est}, Δ', and Δ^{est} recognized using Algorithm 1 and 2. Firstly, the incoming data symbols are shifted by ϕ bit positions, where $\phi = 0 : \Delta' - 1$ and $\Delta' = n \cdot \beta$. For instance, if the receiver starts receiving the turbo convolutional coded data symbols at δth bit position, then time synchronization can be achieved by shifting $\phi^{\text{est}} = (\Delta' - \delta) + 1$ bit positions. This is because, the second RSC encoder operates on a block interleaved sequence with interleaver period $\beta = N_r \times N_c$ and only at every multiples of Δ' bit positions, all the parity bits corresponding to block interleaved message bits will be generated from second RSC encoder. Hence, the maximum range of bit position adjustment parameter is restricted to Δ' as given in Algorithm 3. Since N_r and N_c are hidden inside Δ^{est}, the possible combinations of two factors N'_r and N'_c that satisfy $N'_r \times N'_c = \frac{\Delta_{\text{est}}}{M}$, where $M = 1 : k^{\text{est}}$, are obtained after shifting ϕ bit positions. Similarly, the possible combinations of n'_1 and n'_2, where $n'_1 > 1$ and $n'_2 > 1$, that satisfy $n'_1 + n'_2 = n^{\text{est}} + k^{\text{est}}$ are also obtained. As k^{est} bits are punctured, the total codeword length of two RSC encoders (without puncturing) is equal to $n + k$ i.e. $n_1 + n_2 = n + k$. So we obtain possible combinations of n'_1 and n'_2 that satisfy $n'_1 + n'_2 = n^{\text{est}} + k^{\text{est}}$ to identify individual codeword lengths of RSC encoders.

Algorithm 2: Estimation of code word length, code dimension, and rank deficiency difference parameters (Erroneous conditions).

Notations: Let us denote the column echelon form of data matrix S_j as F_j, j denotes the iteration number, N denotes the number of iterations, $\omega_j(c)$ denotes the ratio of zero elements in cth column of F_j, $\gamma(c)$ denotes the average of $\omega_j(c)$ over N iterations, and $data(\cdot)$ refers to an array of incoming turbo convolutional coded binary data symbols.;
Input: Turbo convolutional coded binary data symbols;
Output: n^{est}, k^{est}, and Δ^{est};
Assumptions: $a \geq b$;
1:**for** $b = b_{min} : b_{max}$ **do**
  2:**for** $j = 1 : N$ **do**
    3: $R_j = data(1 + (j-1)b : ba + (j-1)b)$;
    4: Reshape R_j into a matrix S_j of size $a \times b$;
    5: Convert S_j into F_j using Gauss elimination process;
    6: Compute $\omega_j(c)$ in each column of F_j, where $c \in \{1, 2, ..., b\}$;
    7: Form a row vector $A_j = [\omega_j(1) : \omega_j(b)]$;
  end
  8: Accumulate all the row matrices into a single matrix A of size $N \times b$, where $A = [A_1 ; A_2 ; A_3 ; \cdots A_N]$;
  9: Compute $B = mean(A)$, where $B = [\gamma(1) : \gamma(b)]$ and $\gamma(c) = \frac{\sum_{j=1}^{N} \omega_j(c)}{N}$;
  10: Evaluate $\rho(S)$ as follows: $\rho(S) = \textbf{card}\left(c \in \{1, 2, ..., b\} \mid \gamma(c) < \Gamma_{\text{opt}}^{\text{th}}\right)$ and $p(S) = \frac{\rho(S)}{b}$;
end
11: Execute step 5 to 10 in Algorithm 1 to estimate the code and interleaver parameters n^{est}, k^{est}, and Δ^{est};

The systematic bits can be isolated based on k^{est} and n^{est}. After that based on n'_1 and n^{est}, the bit sequence of the first RSC encoder is grouped. It is also essential to interleave the systematic bits using different values of N'_r and N'_c to identify N_r and N_c. The interleaved systematic bits are combined with the parity sequence of the second RSC encoder based on n'_2. The combined bit sequence is reshaped into a data matrix S_2 of size $a \times b$, where b is fixed as a multiple of n'_2. After reshaping, the estimate of codeword lengths of first and second RSC encoders n_1^{est} and n_2^{est}, bit position adjustment parameter ϕ^{est}, and interleaver parameters N_r^{est} and N_c^{est} are obtained from the corresponding combination $[n'_1, n'_2, N'_r, N'_c, \phi]$ that minimizes rank ratio $p(n'_1, n'_2, N'_r, N'_c, \phi)$ (non-erroneous scenario) and maximizes zero-mean-ratio $\mu(n'_1, n'_2, N'_r, N'_c, \phi)$ (erroneous scenario). In the case of erroneous scenario, the zero-mean-ratio $\mu(n'_1, n'_2, N'_r, N'_c, \phi)$ of column echelon form of S_2 is evaluated instead of rank ratio for different values of n'_1, n'_2, N'_r, N'_c, and ϕ. Zero-mean-ratio is defined as the average of ratio of zero elements over N iterations $\gamma(c)$ to the total number of columns in S_2 i.e. $\mu(n'_1, n'_2, N'_r, N'_c, \phi) = \frac{\sum_{c=1}^{b} \gamma(c)}{b}$. Since dependent and independent columns are classified based on $\gamma(c)$ in Algorithm 2, it is intuitive that the rank deficient and full rank data matrices can be classified based on zero-mean-ratio [12]. The zero-mean-ratio of the column echelon form of rank deficient data matrix will be greater than the full rank data matrix. Therefore, the corresponding combination $[n'_1, n'_2, N'_r, N'_c, \phi]$ that maximizes $\mu(n'_1, n'_2, N'_r, N'_c, \phi)$ is chosen as the estimated parameters as given in step 11 of Algorithm 3.

The code dimensions k_1^{est} and k_2^{est} of the first and second constituent convolutional encoders, respectively, are estimated using Algorithm 4. After recognizing, n_1^{est} and n^{est}, the systemic and parity bit sequences of the first RSC encoder are grouped by shifting ϕ^{est} bit positions. After that the grouped information sequence is reshaped into a data matrix S_1 of size $a_1 \times b_1$ and the rank and rank ratio values are evaluated by varying b_1. It is to be noted that

Algorithm 3: Estimation of interleaver, synchronization parameters, and codeword lengths of individual RSC encoder.

Notations: $\mu(\cdot)$ denotes the zero-mean-ratio;
Assumptions: $a \geq b$ and $\phi \in \{0, \Delta' - 1\}$;
Input: n^{est}, k^{est}, Δ', and Δ^{est};
Output: n_1^{est}, n_2^{est}, N_r^{est}, N_c^{est}, and ϕ^{est};
1:**for** $\phi = 0 : \Delta' - 1$ **do**
2: Shift the incoming binary data symbols by ϕ bit positions;
3:**for** $M = 1 : k^{est}$ **do**
4: Get all possible combinations of two factors N_r' and N_c' such that $N_r' \times N_c' = \frac{\Delta_{\text{est}}}{M}$;
end
5: Get all possible combinations of two values n_1' and n_2' such that $n_1' + n_2' = n^{\text{est}} + k^{\text{est}}$;
6: Based on k^{est} and n^{est}, the systematic bits are isolated;
7: Interleave the systematic bits using N_r' and N_c';
8: Based on n_1', n_2', n^{est}, and k^{est}, group the interleaved systematic and parity bit sequences of second RSC encoder and reshape the information sequence into a matrix S_2 of size $a \times b$, where b is fixed as a multiple of n_2';
9: Evaluate $\gamma(c)$ considering N different iterations similar to Algorithm 2;
10: Calculate zero-mean-ratio $\mu(n_1', n_2', N_r', N_c', \phi)$ of column-echelon form of S_2 for all possible values of n_2', n_2', N_r', N_c', and ϕ, where $\mu(n_1', n_2', N_r', N_c', \phi) = \frac{\sum_{c=1}^{b} \gamma(c)}{b}$;
end
11: Estimate the codeword lengths of first and second RSC encoders, block interleaver, and synchronization parameters as follows:
$[n_1^{\text{est}}, n_2^{\text{est}}, N_r^{\text{est}}, N_c^{\text{est}}, \phi^{\text{est}}] = \underset{n_1', n_2', N_r', N_c', \phi}{\operatorname{argmax}} (\mu(n_1', n_2', N_r', N_c', \phi))$;

the rank and rank ratio values for non-erroneous scenario are obtained from the number of non-zero columns of column echelon form as mentioned in Algorithm 1. Further, in case of erroneous scenario, the rank and rank ratio values are obtained by identifying the independent columns based on $\gamma(c)$ as mentioned in Algorithm 2. From the rank values, the code dimension of the first RSC encoder is estimated by observing the difference between successive rank values corresponding to the rank deficient columns as shown in steps 6 and 7 of Algorithm 4. To estimate the code dimension k_2^{est} of the second RSC encoder, the systematic bits are interleaved using N_r^{est} and N_c^{est}. Further, the interleaved bit sequence is combined with the parity bit sequence of the second RSC encoder based on n_2^{est} and they are reshaped into a data matrix S_2 of size $a_2 \times b_2$. The rank and rank ratio values for both non-erroneous and erroneous channel conditions are evaluated by varying b_2 and the code dimension is recognized similar to first RSC encoder by observing the difference between successive rank values with respect to rank deficient columns as shown in steps 8 to 14 of Algorithm 4.

The following observations are noticed regarding the rank values of individual RSC encoders. The reasons for deficient rank and full rank have been already discussed as well as depicted using Fig. 5(a) and (b). For detailed explanation with case study, [12] can be referred. Let S_i be a data matrix of coded symbols with b_i columns, where i=1 and 2. If $b_i = \alpha \cdot n_i$, then the deficient rank of S_i for convolutional code is given by

$$\rho_i(S_i) = \alpha \cdot k_i + m_i < b_i \,. \tag{11}$$

and if $b_i \neq \alpha \cdot n_i$, then rank of S_i is given by

$$\rho_i(S_i) \leq b_i \,. \tag{12}$$

The rank ratio of S_i is given by $p(S_i) = \frac{\rho(S_i)}{b_i}$.

Let $b_i = \alpha \cdot n_i$ and $b_i' = (\alpha + 1) \cdot n_i$ indicate the two successive columns corresponding to rank deficient matrices and the difference $b_i' - b_i$ gives the value of n_i. Furthermore, the difference between two successive deficient rank values i.e. $(\alpha + 1) \cdot k_i + m_i - (\alpha \cdot k_i + m_i)$ gives the value of k_i as mentioned in Algorithm 4.

Algorithm 4: Estimation of k_1^{est} and k_2^{est}.

Notations: $p_i(\cdot)$ and $\rho_i(\cdot)$ denote the rank ratio and rank, respectively, where i=1 and 2;
Assumptions: $a_i \geq b_i$;
Input: n_1^{est}, n_2^{est}, N_r^{est}, N_c^{est}, and ϕ^{est};
Output: k_1^{est} and k_2^{est};
1:**for** $b_1 = b_{min} : b_{max}$ **do**
2: Based on n_1^{est} and n_{est}, group the systematic and parity bit sequences of first convolutional encoder by shifting ϕ^{est} bit positions;
3: Reshape the coded information sequence of first RSC encoder into a matrix S_1 of size $a_1 \times b_1$;
4: Convert S_1 into column-echelon form F_1 using Gauss elimination process;
5: Evaluate $\gamma(c)$ as given in steps 2 to 9 of Algorithm 2 and calculate $\rho_1(S_1)$ and $p_1(S_1)$ as follows:
$\rho_1(S_1) = \textbf{card}\left(c \in \{1, 2, ..., b_1\} \mid \gamma(c) < \Gamma_{\text{opt}}^{\text{th}}\right)$ and $p_1(S_1) = \frac{\rho_1(S_1)}{b_1}$;
end
6: Observe the difference between successive rank values corresponding to the rank deficient columns and accumulate the values in a row vector D;
7: Estimate code dimension k_1^{est} from the most frequent value in the row vector D;
8:**for** $b_2 = b_{min} : b_{max}$ **do**
9: Based on n_2^{est}, n^{est}, k^{est}, N_r^{est}, and N_c^{est}, interleave the systematic bits and group the interleaved systematic and parity bit sequences of second convolutional encoder by shifting ϕ^{est} bit positions;
10: Reshape the coded information sequence into a matrix S_2 of size $a_2 \times b_2$;
11: Convert S_2 into column-echelon form F_2 using Gauss elimination process;
12: Evaluate $\gamma(c)$ as given in steps 2 to 9 of Algorithm 2 and calculate $\rho_2(S_2)$ and $p_2(S_2)$ as follows:
$\rho_2(S_2) = \textbf{card}\left(c \in \{1, 2, ..., b_2\} \mid \gamma(c) < \Gamma_{\text{opt}}^{\text{th}}\right)$ and $p_2(S_2) = \frac{\rho_2(S_2)}{b_2}$;
end
13: Observe the difference between successive rank values corresponding to the rank deficient columns and accumulate the values in a row vector E;
14: Estimate code dimension k_2^{est} from the most frequent value in the row vector E;

After substituting $b_i = \alpha \cdot n_i$, (11) can be written as

$$\alpha \cdot k_i + m_i < \alpha \cdot n_i \,. \tag{13}$$

After rearranging, (13) can be written as

$$\alpha \cdot n_i \cdot \left(1 - \frac{k_i}{n_i}\right) > m_i \,, \tag{14}$$

$$\alpha \cdot n_i > \frac{n_i}{n_i - k_i} m_i \,, \tag{15}$$

$$\alpha > \frac{m_i}{(n_i - k_i)} \,. \tag{16}$$

Now the minimum value of α, which is denoted by α_{min}, is given by

$$\alpha_{\text{min}} = \left\lfloor \frac{m_i}{(n_i - k_i)} \right\rfloor + 1 \,, \tag{17}$$

where $\lfloor x \rfloor$ indicates floor(x). From (17), b_{min} is given by

$$b_i^{\text{min}} = \left(\left\lfloor \frac{m_i}{(n_i - k_i)} \right\rfloor + 1 \right) \cdot n_i \tag{18}$$

After evaluating rank $\rho_i(\cdot)$ and rank ratio $p_i(\cdot)$ of individual RSC encoders from rank deficiency plots for different values of b_i, observe the minimum value of the number of columns with which the data matrix S_i would have deficient rank for the first time and let us denote the same by b_i^{min}. It is observed that b_i^{min} obtained using simulations exactly matches with (18) and the same is tabulated in Table 1. The octal representation of generator sequence is denoted by g_i. It has been observed that there exits a one-to-one correspondence between b_i^{min} and constraint length K_i as shown

Table 1
Minimum number of columns required to obtain the first rank deficient matrix for different convolutional codes.

r_i	n_i	k_i	K_i	$b_i^{\min}$	g_i (octal representation)
			3	6	[5/7, 1]
			4	8	[15/17, 1]
			5	10	[23/35, 1]
			6	12	[57/65, 1]
1/2	2	1	6	12	[53/75, 1]
			7	14	[133/171, 1]
			8	16	[237/345, 1]
			9	18	[561/753, 1]
			10	20	[1167/1545, 1]
			11	22	[2335/3661, 1]
1/3	3	1	4	6	[13/17, 15/17, 1]
			7	12	[133/171, 165/171, 1]
			10	15	[1117/1633, 1365/1633, 1]
1/4	4	1	7	12	[115/174, 136/174, 162/174, 1]
			10	16	[1115/1651, 1363/1651, 1632/1651, 1]

in Table 1. Hence, in a nutshell, constraint length K_i of individual RSC encoders can be estimated from $b_i^{\min}$.

Otherwise, the constraint length K_i is calculated as follows: By plotting rank $\rho_i(S_i)$ with respect to b_i, we can estimate the values of code parameters (i.e. k_i^{est} and n_i^{est}) of individual RSC encoders (refer to Algorithm 3 and 4). From (11), the memory of ith RSC encoder can be written as

$$m_i = \rho_i(S_i) - \alpha \times k_i \,. \tag{19}$$

By substituting $\alpha = b_i/n_i$, the memory of ith RSC encoder is estimated as

$$m_i^{\text{est}} = \rho(S_i) - \frac{b_i \times k_i^{\text{est}}}{n_i^{\text{est}}} \,. \tag{20}$$

Considering $r = 1/n$ convolutional codes, the constraint length of ith RSC encoder is given by $K_i^{\text{est}} = m_i^{\text{est}} + 1$.

6. Simulation results and discussions

Let us denote the first and second RSC encoders as $C(n_i, k_i, K_i)[g_i]$, where $i = 1$ and 2, for rate k_i/n_i code. In the proposed algorithms for erroneous scenario (i.e. Algorithm 2), it is to be noted that the rank values are evaluated based on a fixed threshold. The optimal threshold value $\Gamma_{\text{opt}}^{\text{th}}$ is fixed by plotting the histogram for ratio of zero elements $B = mean(A)$, where $B = [\gamma(1) : \gamma(b)]$, considering particular number of columns b that results in rank deficiency. A range of possible threshold values that properly classify the dependent and independent columns are obtained from the histogram plots. A safe optimal threshold value $\Gamma_{\text{opt}}^{\text{th}}$ is chosen from the range of possible values. In addition, the optimal threshold value can also be obtained through analytical approach (refer to [12, eq. (25)]). The analytical and histogram approaches are investigated in detail for setting the optimal threshold value to evaluate the rank in [12]. It has been identified that the histogram approach performs better than the analytical approach for noisy environment and the optimal threshold values are tabulated for different convolutional codes (refer to Table II in [12]).

Since turbo convolutional encoder is constructed using two convolutional encoders, the optimal threshold values obtained for convolutional codes are also valid for TCCs. From the tabulated values in [12], we fixed $\Gamma_{\text{opt}}^{\text{th}} = 0.55$ for $a = 20 \times b$ to estimate TCC parameters. Note that $\Gamma_{\text{opt}}^{\text{th}}$ is dependent on the number of rows a. For instance, when $a = 5 \times b$, it has been noted that the probability of correct estimation is more than 80% when $\Gamma_{\text{opt}}^{\text{th}} = 0.65, 0.67$, and 0.69. Since compared to other threshold values, the probability

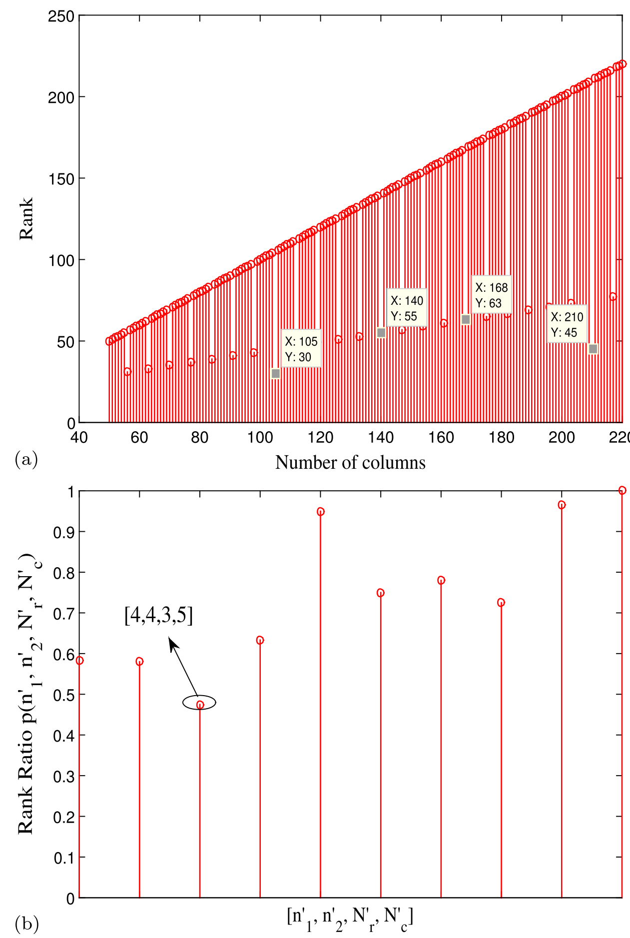

Fig. 6. (a) Variation of rank values with respect to number of columns for TCC considering QPSK scheme, $C(4,1,7)$, $C(4,1,10)$, $N_r = 3$, and $N_c = 5$ for non-erroneous scenario. (b) Variation of rank ratio $p(n_1', n_2', N_r', N_c')$ with respect to $[n_1', n_2', N_r', N_c']$ for TCC considering QPSK scheme, $C(4,1,7)$, $C(4,1,10)$, $N_r = 3$, and $N_c = 5$ for non-erroneous scenario.

of correct estimation is higher for these three values, we have assumed one of the threshold value i.e. $\Gamma_{\text{opt}}^{\text{th}} = 0.65$ in our Algorithms for the case when $a = 5 \times b$. In addition, we fixed number of iterations $N = 100$ in Algorithm 2 to identify parameters over erroneous scenario. It is intuitive that the increase in number of iterations N and number of rows a improve the accuracy of estimation. It is also to be noted that the values of $b_{\min}$ and $b_{\max}$ used in our algorithms are not known at the receiver. We have fixed the range in such a way that we obtain at least two deficient rank values to evaluate the code parameters. If required rank deficient values are not obtained within the fixed range, then we increase the range accordingly.

In Fig. 6(a), the variation of rank values with respect to number of columns b is shown for TCC considering two non-identical RSC encoders $C(4,1,7)[115/174, 136/174, 162/174, 1]$ and $C(4,1,10)[1115/1651, 1363/1651, 1632/1651, 1]$ with a block interleaver assuming $N_r = 3$, $N_c = 5$, quadrature phase-shift keying (QPSK), non-erroneous, and synchronized scenario. The rank values are evaluated using Algorithm 1. From the figure, the difference between successive number of columns with deficient rank values gives the value of codeword length of TCC i.e. $n^{\text{est}} = n_1 + n_2 - k = 7$. Further, the code dimension is estimated as $k^{\text{est}} = 1$ from the deficient rank values. By observing the difference between non-contiguous deficient rank values (at $b = 105$ and $b = 210$), Δ' and Δ^{est} are identified as 105 and 15, respectively. The non-contiguous deficient rank values corresponding to $b = 105$ and $b = 210$ match with the rank expression given by (8). Similarly, the deficient

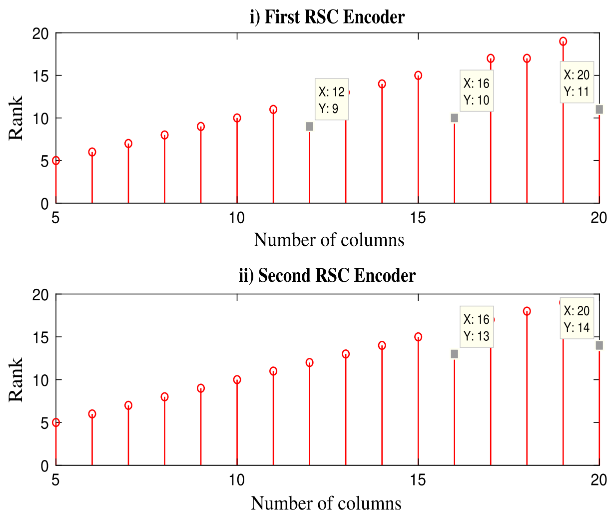

Fig. 7. Variation of rank values with respect to number of columns for individual RSC encoders.

rank values corresponding to $b=140$ and $b=168$ validate (6). According to Algorithm 3, the rank ratio values are calculated for all possible combinations of N_r', N_c', n_1', and n_2' by fixing b as a multiple of n_2'. It has been noticed from Fig. 6(b) that for $[n_1', n_2', N_r', N_c'] = [4, 4, 3, 5]$, the rank ratio value $p(n_1', n_2', N_r', N_c')$ is minimum. Hence, the code and interleaver parameters $n_1^{est}=4$, $n_2^{est}=4$, $N_r^{est}=3$, and $N_c^{est}=5$ are correctly identified using Algorithm 1 and 3.

In Fig. 7, the variation of rank with respect to number of columns is shown for individual RSC encoders. Here, the rank values are evaluated using Algorithm 4. It has been observed from both the plots that the difference between successive number of columns with rank deficiency is equal to 4 for both RSC encoders, which validate the codeword lengths $n_1^{est}=4$ and $n_2^{est}=4$ estimated from Fig. 6(b). By observing the difference between the rank values corresponding to the rank deficient columns, code dimensions of individual RSC encoders i.e. $k_1^{est}=1$ and $k_2^{est}=1$ are identified successfully using Algorithm 4. From the plots, it is also noticed that $b_1^{min}=12$ (plot i) and $b_2^{min}=16$ (plot ii). From the tabulated values in Table 1, $b_i^{min}=12$ and 16 correspond to constraint lengths $K_1^{est}=7$ and $K_2^{est}=10$, respectively, of rate 1/4 convolutional code and the same match with the constraint lengths assumed for transmission.

In Fig. 8(a), the variation of rank with respect to number of columns b is shown for TCC considering two non-identical RSC encoders $C(3, 1, 7)[133/171, 165/171, 1]$ and $C(2, 1, 7)[133/171, 1]$ with a block interleaver $N_r=4$ and $N_c=3$ assuming 16-QAM scheme, symbol error rate (SER) $=5\times10^{-3}$, and delay $\delta=8$ bit positions. The rank values are evaluated based on Algorithm 2, which is proposed for erroneous scenario. From the figure, the difference between successive number of columns with rank deficiency gives the value of codeword length $n^{est}=4$. Further, $\hat{\gamma}'=2$ and $k^{est}=1$ are recognized from the rank values corresponding to the rank deficient columns. By noticing the non-contiguous deficient rank values, $\Delta^{est}=12$ is identified and the deficient rank values validate (4) and (8). Further, the zero-mean-ratio values are evaluated for all possible combinations of N_r', N_c', n_1', and n_2' by shifting ϕ bit positions as mentioned in Algorithm 3. It has been noticed from the Fig. 8(b) that for $[n_1', n_2', N_r', N_c', \phi] = [3, 2, 4, 3, 41]$, zero-mean ratio $\mu(n_1', n_2', N_r', N_c', \phi)$ reaches maximum. Therefore, the code and interleaver parameters $n_1^{est}=3$, $n_2^{est}=2$, $N_r^{est}=4$, and $N_c^{est}=3$ are successfully identified for erroneous scenario. In addition, the bit adjustment parameter $\phi^{est}=(\Delta'-\delta)+1=41$ to achieve time synchronization is also identified correctly for non-synchronized scenario.

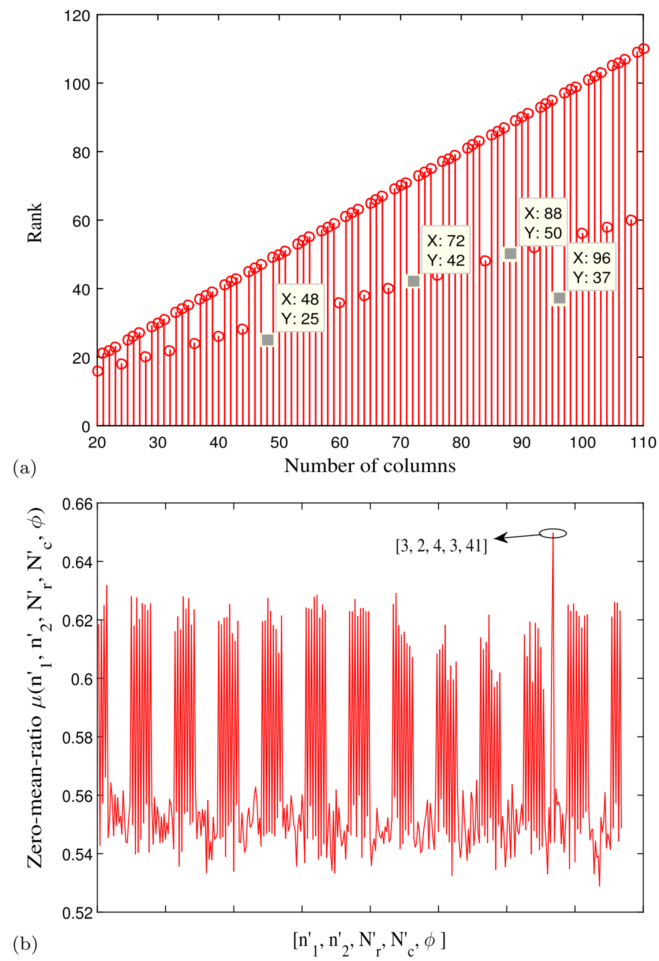

Fig. 8. (a) Variation of rank values with respect to number of columns for TCC considering 16-QAM scheme, $C(3, 1, 7)$, $C(2, 1, 7)$, $N_r=4$, and $N_c=3$ assuming SER=5×10^{-3} and delay $\delta=8$ (b) Variation of zero-mean-ratio $\mu(n_1', n_2', N_r', N_c', \phi)$ with respect to $[n_1', n_2', N_r', N_c', \phi]$ for TCC considering 16-QAM scheme, $C(3, 1, 7)$, $C(2, 1, 7)$, $N_r=4$, and $N_c=3$ assuming SER=5×10^{-3} and delay $\delta=8$.

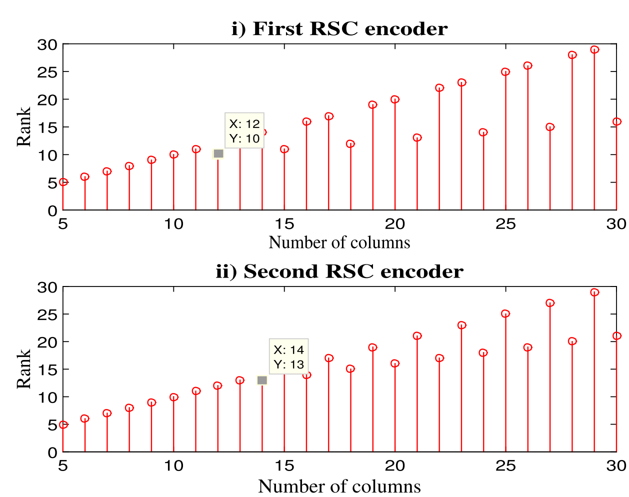

Fig. 9. Variation of rank values with respect to number of columns for individual RSC encoders.

The variation of rank with respect to number of columns b_i is shown in Fig. 9 for individual RSC encoders and the rank values are evaluated using Algorithm 4. It is observed from the plots

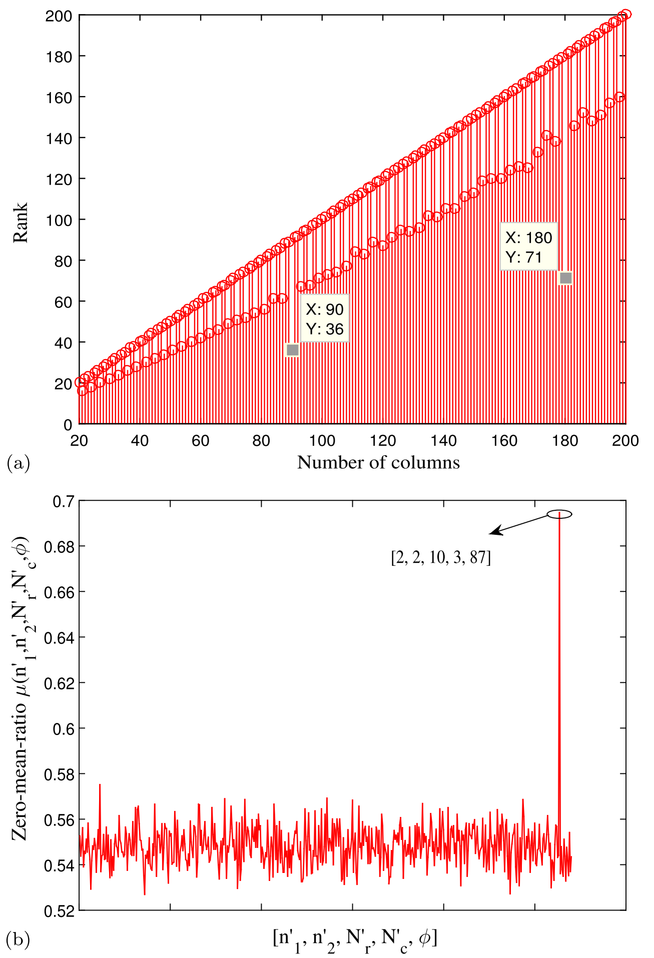

Fig. 10. (a) Variation of rank values with respect to number of columns for TCC considering 16-QAM scheme, $C(2,1,3)$, $C(2,1,5)$, $N_r = 10$, $N_c = 3$, SER=10^{-2}, and $\delta = 4$ (b) Variation of zero-mean-ratio $\mu(n'_1, n'_2, N'_r, N'_c, \phi)$ with respect to $[n'_1, n'_2, N'_r, N'_c, \phi]$ for TCC considering 16-QAM scheme, $C(2,1,3)$, $C(2,1,5)$, $N_r = 10$, $N_c = 3$, SER=10^{-2}, and $\delta = 4$.

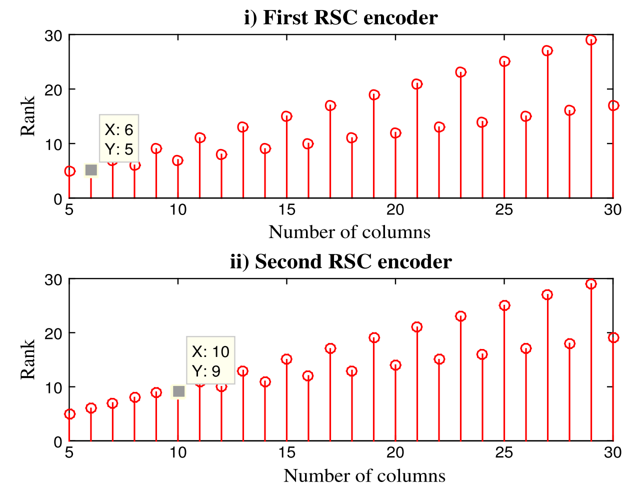

Fig. 11. Variation of rank values with respect to number of columns for individual RSC encoders.

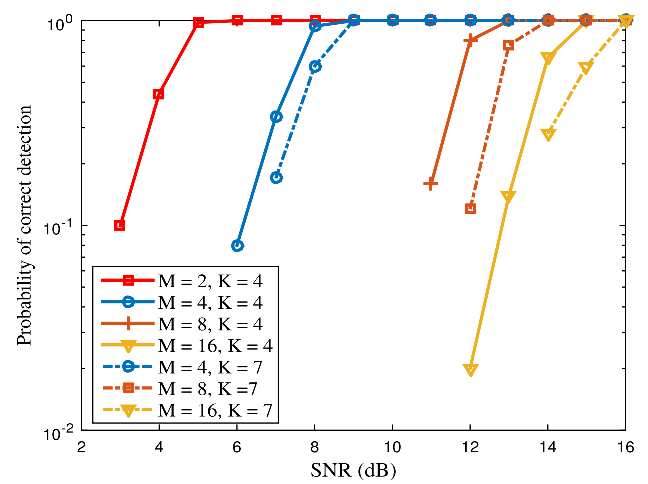

Fig. 12. Accuracy of estimation of code and interleaver parameters for two different TCCs $C(3,1,4)$ and $C(3,1,7)$ assuming identical RSC encoders with a block interleaver $N_r = 3$ and $N_c = 5$ for different $M-$QAM schemes.

that the codeword lengths $n_1^{est} = 3$ and $n_2^{est} = 2$ of individual RSC encoders are identified correctly. From the difference between the rank values corresponding to the rank deficient columns, code dimensions of individual RSC encoders i.e. $k_1^{est} = k_2^{est} = 1$ are identified successfully. It is also noticed from the figure that $b_1^{min} = 12$ (plot i) and $b_2^{min} = 14$ (plot ii). From the tabulated values, it is inferred that $b_1^{min} = 12$ for rate 1/3 convolutional codes and $b_2^{min} = 14$ for rate 1/2 convolutional codes correspond to constraint lengths $K_1^{est} = K_2^{est} = 7$ and they match with the constraint lengths assumed for transmission.

In Fig. 10(a), the variation of rank with respect to the number of columns is shown for TCC considering two non-identical RSC encoders $C(2,1,3)[5/7,1]$ and $C(2,1,5)[23/35,1]$ with a block interleaver assuming $N_r = 10$, $N_c = 3$, SER=10^{-2}, 16-QAM scheme, and $\delta = 4$ bit positions. From the figure, the difference between successive number of columns with rank deficiency gives the codeword length of TCC i.e. $n^{est} = 3$. From the rank values corresponding to the rank deficient columns, $k^{est} = 1$ is recognized correctly. From the non-contiguous deficient rank values, Δ' and Δ^{est} are identified as 90 and 30, respectively. Further, it has also been observed that $\mu(n'_1, n'_2, N'_r, N'_c, \phi)$ is maximum for $[n'_1, n'_2, N'_r, N'_c, \phi] = [2, 2, 10, 3, 87]$ as shown in Fig. 10(b). Hence, the estimated code and interleaver parameters are as follows: $n_1^{est} = 2$, $n_2^{est} = 2$, $N_r^{est} = 10$, $N_c^{est} = 3$, and $\phi^{est} = 87$.

It is to be noted from Fig. 8(a) and 10(a) that few deficient and non-contiguous rank values are greater than the bounds given by (4) and (8). This is because, it is difficult to classify all dependent and independent columns correctly for more erroneous channel conditions. Hence, we adopt maximum likelihood approach to successfully identify parameters by choosing the most frequent value from the accumulated values in the row vectors as mentioned in our Algorithms.

In Fig. 11, the variation of rank values with respect to number of columns b_i is shown for individual RSC encoders. From both the plots, the difference between successive number of columns with rank deficiency is equal to 2. Hence, codeword lengths $n_1^{est} = 2$ and $n_2^{est} = 2$ are estimated correctly using Algorithm 4. Therefore, the codeword lengths of individual RSC encoders identified using Algorithm 3 are validated using Algorithm 4. In addition, by observing the difference between the rank values corresponding to the rank deficient columns, code dimensions of individual RSC encoders i.e. $k_1^{est} = k_2^{est} = 1$ are identified successfully. It is also inferred that $b_i^{min} = 6$ and 10 from plots i and ii correspond to constraint lengths $K_1^{est} = 3$ and $K_2^{est} = 5$, respectively, as given in Table 1. Thus, the constraint length values of individual RSC encoders are also successfully estimated for the case when SER=10^{-2}.

In Fig. 12, the probability of correct estimation of code and interleaver parameters is shown for two different TCCs 1) $C(3,1,4)$

[13/17, 15/17, 1] and 2) $C(3, 1, 7)[133/171, 165/171, 1]$ assuming identical RSC encoders with a block interleaver $N_r = 3$ and $N_c = 5$ for different $M-$QAM schemes, where M denotes the modulation order. Firstly, from the plots it is inferred that the accuracy of estimation is 100% for $M = 2$, 4, 8, and 16 when SNR $\geq$ 5, 9, 13, and 15 dB, respectively, for constraint length $K = 4$. Hence, the accuracy of estimation deteriorates with increase in M, as expected. It is also observed from the figure that the accuracy of estimation is 100% for $M = 4$, 8, and 16 when SNR $\geq$ 9, 14, and 16 dB, respectively, for $K = 7$. Thus, the accuracy of estimation deteriorates with increase in M similar to $K = 4$ case. Further, increase in constraint length K deteriorates the performance and it is mainly due to difficulty in identifying dependent columns. The rank values will increase and the number of dependent columns will decrease with increase in constraint length. Hence, it is always a challenging process to identify less number of dependent columns over erroneous channel conditions.

The existing methods proposed for TCCs in [17] and [18] were restricted to the blind reconstruction of first RSC encoder without reconstructing the second RSC encoder and interleaver. In addition, critical parameter like constraint length is assumed to be known at the receiver and the algorithms were limited only to synchronized environment. The existing method in [17] achieves 95% accuracy at SNR = 12 dB to reconstruct first RSC encoder $C(2, 1, 4)[15/17, 1]$ considering binary phase-shift keying (BPSK) scheme. In [20], the proposed method estimates total codeword length and code dimension of TCC considering two identical RSC encoders $C(2, 1, 4)$ with almost 100% accuracy at SNR = 5.2 dB. However, the proposed algorithms in our work identify code parameters of two identical RSC encoders $C(2, 1, 4)[15/17, 1]$, interleaver parameters of block interleaver with $N_r = 3$, $N_c = 4$, and bit position adjustment parameter to achieve frame synchronization with 98% accuracy at SNR = 5 dB considering BPSK scheme. Hence, the proposed methods recognize the parameters of two RSC encoders and block interleaver and achieve frame synchronization with significant improvement in accuracy compared to the existing expectation-maximization (EM) method [17], which identifies only first RSC encoder parameters. In addition, the proposed algorithms achieve almost equivalent performance as that of existing method in [20]. As mentioned before, the algorithm proposed in [20] estimates only total codeword length and code dimension of TCCs assuming two identical RSC encoders without estimating the parameters of constituent RSC encoders and interleavers. We estimate the total codeword length and code dimension of TCCs over non-erroneous and erroneous channel conditions using Algorithms 1 and 2, respectively. The estimated parameters from Algorithm 2 are given as inputs for Algorithms 3 and 4 to achieve frame synchronization and to estimate individual constituent RSC encoder and interleaver parameters. Finally, the superiority of the proposed algorithms compared to the existing algorithms lies in the blind estimation of two non-identical RSC encoder and interleaver parameters of TCCs along with achieving frame synchronization. To the best of our knowledge, none of the existing methods have reconstructed all the blocks of turbo convolutional encoder over erroneous channel conditions.

Due to high computational complexity of Gauss elimination process, applications of the proposed algorithms will have limitations in real-time AMC systems, reconfigurable radio systems, etc. The proposed algorithms are mainly suitable for non-cooperative military and spectrum surveillance systems, where complexity is not a major concern. As a part of our future work, the proposed algorithms will be modified by reducing the computational complexity to estimate the code parameters of practical real-time AMC-based communication systems and reconfigurable radio systems.

7. Conclusions

In this paper, the blind reconstruction algorithms for TCC are proposed for noisy environment. We consider parallel concatenation of two RSC encoders with a matrix-based block interleaver. The estimated code and interleaver parameters are grouped as follows: 1) codeword length and code dimension of TCC 2) codeword lengths, code dimensions and constraint lengths of individual RSC encoders 3) rank deficiency difference, number of rows and columns of block interleaver matrix. Apart from the code and interleaver parameters, the bit position adjustment parameter is also identified using the proposed algorithms in order to achieve frame synchronization. It is observed from the simulation results that the code, interleaver, and synchronization parameters are successfully recognized for various test cases. Further, in order to show the robustness of the proposed algorithms, the performance in terms of accuracy of estimation is investigated for various M-QAM schemes and constraint length values. It is inferred that the accuracy of estimation improves with decrease in modulation order and constraint length. Finally, the proposed algorithm, which recognizes the parameters of two RSC encoders and block interleaver, for noisy environment outperforms the existing algorithm proposed in the prior work.

Declaration of competing interest

The authors declare that they have no known competing financial interests or personal relationships that could have appeared to influence the work reported in this paper.

Appendix A. Case study 1

For better understanding, a case study explaining the rank deficiency and full rank phenomena of TCC for the case when $n_2 - k_2 = 1$ has been discussed in this Appendix.

Let us assume that the input data sequence $(d_1, d_2, d_3, d_4, \cdots)$ enters the turbo convolutional encoder comprising of two RSC encoders $C(2, 1, 3)[5/7, 1]$ and $C(2, 1, 3)[5/7, 1]$ with a block interleaver assuming $N_r = 3$ and $N_c = 2$ one bit at a time. The output of the first RSC encoder corresponding to the data sequence is given by $(d_1, p_1, d_2, p_2, d_3, p_3, d_4, p_4, \cdots)$, where (p_1, p_2, p_3, p_4) are the parity bits corresponding to (d_1, d_2, d_3, d_4). Similarly, (q_1, q_2, q_3, q_4) are the parity bits corresponding to the interleaved input sequence and the same is the output of the second RSC encoder as shown in Fig. 3. Thus, the final output sequence of rate $r = 1/3$ turbo convolutional encoder is given by $(d_1, p_1, q_1, d_2, p_2, q_2, d_3, p_3, q_3, d_4, p_4, q_4, \cdots)$. For this test case, it is to be noted that $n = 3$, $k = 1$, $m_1 = 2$, and $m_2 = 2$. The final output sequence is reshaped into a data matrix S of size $a \times b$ assuming $b = 9, 10, 12, \text{and}, 18$ as shown in Table A.2. Note that for better understanding we have shown only three rows of data matrix S. However, we have assumed $a \geq b$ in the Algorithm to obtain rank values lesser than or equal to b. It is also to be noted that the rank versus number of columns plot is also shown for the assumed test case in Fig. A.13.

From Table A.2, it is observed that the data and parity bits are aligned properly in the same column for the case when b is a multiple of $n = 3$ (i.e. $b = 9, 12, \text{and}, 18$). Thus, the linear relationship between data and parity bits will be satisfied across all the rows, which will result in linear relationship between the columns. Hence, rank deficiency will be obtained after converting S into column echelon form F (as mentioned in the Algorithms). This rank deficiency phenomenon is also justified using Fig. A.13, as deficient rank values are obtained for $b = 9, 12, \text{and}, 18$. But for the case when is not a multiple of $n = 3$ (i.e. $b = 10$), the data and parity bits are not aligned properly in the same column. This will

Table A.2
Turbo convolutional coded data assuming $C(2,1,3)[5/7,1]$ and $C(2,1,3)[5/7,1]$ with a block interleaver $N_r=3$ and $N_c=2$.

	d_1	p_1	q_1	d_2	p_2	q_2	d_3	p_3	q_3									
$b=9$	d_4	p_4	q_4	d_5	p_5	q_5	d_6	p_6	q_6									
	d_7	p_7	q_7	d_8	p_8	q_8	d_9	p_9	q_9									
	d_1	p_1	q_1	d_2	p_2	q_2	d_3	p_3	q_3	d_4								
$b=10$	p_4	q_4	d_5	p_5	q_5	d_6	p_6	q_6	d_7	p_7								
	q_7	d_8	p_8	q_8	d_9	p_9	q_9	d_{10}	p_{10}	q_{10}								
	d_1	p_1	q_1	d_2	p_2	q_2	d_3	p_3	q_3	d_4	p_4	q_4						
$b=12$	d_5	p_5	q_5	d_6	p_6	q_6	d_7	p_7	q_7	d_8	p_8	q_8						
	d_9	p_9	q_9	d_{10}	p_{10}	q_{10}	d_{11}	p_{11}	q_{11}	d_{12}	p_{12}	q_{12}						
	d_1	p_1	q_1	d_2	p_2	q_2	d_3	p_3	q_3	d_4	p_4	q_4	d_5	p_5	q_5	d_6	p_6	q_6
$b=18$	d_7	p_7	q_7	d_8	p_8	q_8	d_9	p_9	q_9	d_{10}	p_{10}	q_{10}	d_{11}	p_{11}	q_{11}	d_{12}	p_{12}	q_{12}
	d_{13}	p_{13}	q_{13}	d_{14}	p_{14}	q_{14}	d_{15}	p_{15}	q_{15}	d_{16}	p_{16}	q_{16}	d_{17}	p_{17}	q_{17}	d_{18}	p_{18}	q_{18}

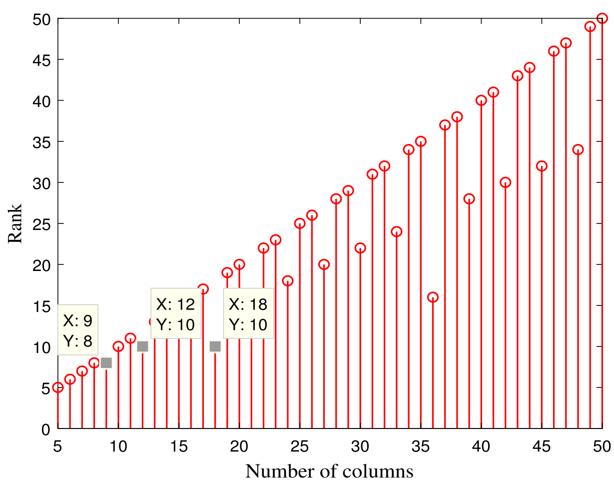

Fig. A.13. Rank versus number of columns plot for test case with two identical RSC encoders $C(2,1,3)[5/7,1]$ and $C(2,1,3)[5/7,1]$ with a block interleaver $N_r=3$ and $N_c=2$.

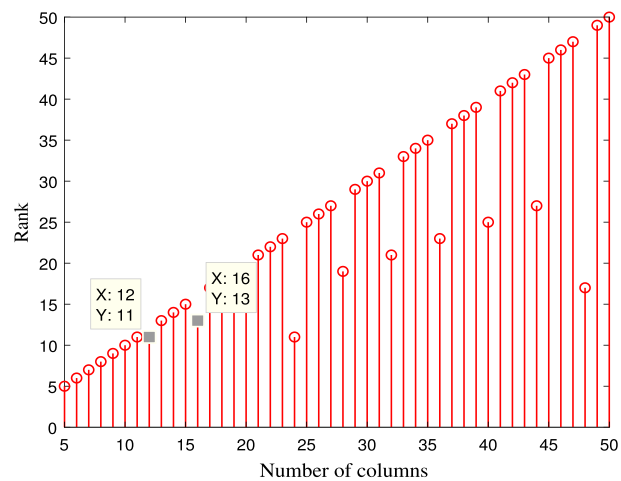

Fig. B.14. Rank versus number of columns plot for test case with two non-identical RSC encoders $C(2,1,3)[5/7,1]$ and $C(3,1,4)[13/17,15/17,1]$ with a block interleaver $N_r=3$ and $N_c=2$.

affect the linear relationship between the columns, which will result in full rank with high probability as shown in Fig. A.13. The obtained full rank value matches with (5).

For convolutional codes, as already mentioned, $\alpha' \cdot n$ output coded bits depend on $\alpha' \cdot k$ present and m_1 previous input bits (i.e. $\alpha \cdot k + m_1$ bits). It is observed that the message and parity bits of $\alpha' = 3$ and 4 codewords are aligned properly in the same column for $b=9$ and 12, respectively. Thus, after converting S into F through Gauss elimination process, there will be only $\alpha' \cdot k + m_1 = 5$ non-zero or independent columns out of $b=9$ columns and 6 independent columns out of $b=12$ columns in the case of first RSC encoder. Since we have taken two identical RSC encoders into consideration with rate $r = 1/2$ and constraint length $K=3$, the memory orders of RSC encoders are given by $m_1 = m_2 = 2$. In addition, the output sequence contains one parity bit from second RSC encoder without message bits (due to puncturing) as $n_2 - k_2 = 1$. This will result in another $\alpha' = 3$ and 4 independent columns for $b=9$ and 12 due to non-existence of linear relations between columns. In a nutshell, we will obtain rank values of 8 and 10 for $b=9$ and 12, respectively, and the same are also validated in Fig. A.13. Thus, the obtained rank values well agree with the rank equation given by (4).

For the case when $b=18$, the data and parity bits of $\alpha' = 6$ codewords are aligned properly in the same column. We assume interleaver period $\beta = N_r N_c = 6$ and it is to be noted that $b=18$ is a multiple of $\Delta' = \beta \cdot n$. As already mentioned, only at multiples $\beta \cdot n$, the parity bits from the second RSC encoder can also be represented as a linear combination of systematic message bits from the first RSC encoder. But for other values of b, only few or no parity bits generated from the second RSC encoder can be represented as a linear combination of message bits due to incomplete interleaving. Thus, the output coded bits from turbo convolutional encoder will be viewed as the bits generated from single convolutional encoder whose memory is equal to $m_1 + m_2 = 4$ for the case when $b=18$. After converting S with $b = \alpha \cdot \Delta' = 18$ columns into F, at most $\beta \cdot \alpha \cdot k + m_1 + m_2 = 10$ non-zero columns out of b columns will be observed as shown in Fig. A.13, where $\alpha = k = 1$. The obtained rank value also well agree with the rank equation given by (8).

Appendix B. Case study 2

In this section, another case study explaining the rank deficiency and full rank phenomena of TCC for the case when $n_2 - k_2 > 1$ has been discussed. Here, we assume the input data sequence enters the turbo convolutional encoder comprising of two non-identical RSC encoders $C(2,1,3)[5/7,1]$ and $C(3,1,4)[13/17,15/17,1]$ with a block interleaver assuming $N_r = 3$ and $N_c = 2$. The data matrix with $b=12$ and $b=16$ is shown in Table B.3 and the rank versus number of columns plot for the same test case is shown in Fig. B.14. Since the assumed RSC encoder is $C(3,1,4)[13/17,15/17,1]$, two parity bits will be generated as the output of the second RSC encoder for each message bit. Thus, the final output sequence of rate $r = 1/4$ turbo convolutional encoder is given by $(d_1, p_1, q_1, q_2, d_2, p_2, q_3, q_4, d_3, p_3, q_5, q_6, d_4, p_4, q_7, q_8, \cdots)$. For this test case, it is to be noted that $n=4$, $k=1$, $m_1=2$, and $m_2=3$. It is observed from Table B.3 that the data and parity bits are aligned properly in the same column for the case when b is a

Table B.3
Turbo convolutional coded data assuming $C(2,1,3)[5/7,1]$ and $C(3,1,4)[13/17,15/17,1]$ with a block interleaver $N_r=3$ and $N_c=2$.

$b=12$	d_1	p_1	q_1	q_2	d_2	p_2	q_3	q_4	d_3	p_3	q_5	q_6				
	d_4	p_4	q_7	q_8	d_5	p_5	q_9	q_{10}	d_6	p_6	q_{11}	q_{12}				
	d_7	p_7	q_{13}	q_{14}	d_8	p_8	q_{15}	q_{16}	d_9	p_9	q_{17}	q_{18}				
$b=16$	d_1	p_1	q_1	q_2	d_2	p_2	q_3	q_4	d_3	p_3	q_5	q_6	d_4	p_4	q_7	q_8
	d_5	p_5	q_9	q_{10}	d_6	p_6	q_{11}	q_{12}	d_7	p_7	q_{13}	q_{14}	d_8	p_8	q_{15}	q_{16}
	d_9	p_9	q_{17}	q_{18}	d_{10}	p_{10}	q_{19}	q_{20}	d_{11}	p_{11}	q_{21}	q_{22}	d_{12}	p_{12}	q_{23}	d_{24}

multiple of $n=4$ (i.e. $b=12$ with $\alpha'=3$ and $b=16$ with $\alpha'=4$). As $\alpha'\cdot(n_2-k_2)=6$ and 8 parity bits from second RSC encoder are aligned properly in the same column for $b=12$ and $b=16$, respectively, they will act as coded bits. Thus, $\alpha'\cdot(n_2-k_2)=6$ columns due to second RSC encoder S will result in $\alpha'\cdot k_2+m_2=6$ independent columns in addition to $\alpha'\cdot k_1+m_1=5$ columns due to first RSC encoder for $b=12$ case. Similarly, $\alpha'\cdot(n_2-k_2)=8$ columns will result in $\alpha'\cdot k_2+m_2=7$ independent columns in addition to $\alpha'\cdot k_1+m_1=6$ columns for $b=16$ case. Therefore, the obtained rank values will be equal to 11 and 13 for $b=12$ and 16, respectively, and they are also justified in Fig. B.14. Finally, the rank values match with the rank equation given by (6).

References

[1] J.F. Ziegler, Automatic Recognition and Classification of Forward Error Correcting Codes, Ph.D. thesis, George Mason University, Fairfax, Virginia (Spring), 2000.

[2] C. Choi, D. Yoon, Enhanced blind interleaver parameters estimation algorithm for noisy environment, IEEE Access 6 (Sep. 2017) 5910–5915, https://doi.org/10.1109/ACCESS.2017.2754638.

[3] M. Marazin, R. Gautier, G. Burel, Dual code method for blind recognition of convolutional encoder for cognitive radio receiver design, in: Proc. IEEE Global Telecommunications Conference (GLOBECOM), 2009, pp. 1–6.

[4] M. Marazin, R. Gautier, G. Burel, Blind recovery of k/n rate convolutional encoders in a noisy environment, EURASIP J. Wirel. Commun. Netw. 2011 (2011) 168, https://doi.org/10.1186/1687-1499-2011-168, 9 pp.

[5] M. Abdelbar, W.H. Tranter, T. Bose, Cooperative cumulants-based modulation classification in distributed networks, IEEE Trans. Cogn. Commun. Netw. 4 (3) (Sep. 2018) 446–461, https://doi.org/10.1109/TCCN.2018.2824326.

[6] T. Xia, H.-C. Wu, Novel blind identification of ldpc codes using average llr of syndrome a posteriori probability, IEEE Trans. Signal Process. 62 (3) (Feb. 2014) 632–640, https://doi.org/10.1109/TCCN.2018.2824326.

[7] H. Zhang, H.-C. Wu, H. Jiang, Novel blind encoder identification of Reed-Solomon codes with low computational complexity, in: Proc. IEEE GLOBECOM, 2013, pp. 3294–3299.

[8] R. Moosavi, E.G. Larsson, Fast blind recognition of channel codes, IEEE Trans. Commun. 62 (5) (May 2014) 1393–1405, https://doi.org/10.1109/TCOMM.2014.050614.130297.

[9] J. Dingel, J. Hagenauer, Parameter estimation of a convolutional encoder from noisy observations, in: Proc. IEEE International Symposium on Information Theory (ISIT), 2007, pp. 1–5.

[10] M. Marazin, R. Gautier, G. Burel, Some interesting dual-code properties of convolutional encoder for standards self-recognition, IET Commun. 6 (8) (July 2012) 931–935, https://doi.org/10.1049/iet-com.2010.0463.

[11] M. Cluzeau, M. Finiasz, Reconstruction of punctured convolutional codes, in: Proc. IEEE Information Theory Workshop, 2009, pp. 75–79.

[12] R. Swaminathan, A.S. Madhukumar, Classification of error correction codes and estimation of interleaver parameters in a robust environment, IEEE Trans. Broadcast. 63 (3) (Sep. 2017) 463–478, https://doi.org/10.1049/iet-com.2010.0463.

[13] Y. Zrelli, R. Gautier, E. Rannou, M. Marazin, E. Radoi, Blind identification of code word length for non-binary error-correcting codes in noisy transmission, EURASIP J. Wirel. Commun. Netw. 2015 (2015) 43, https://doi.org/10.1186/s13638-015-0294-5, 16 pp.

[14] A. Zahedi, G.R. Mohammad-Khani, Reconstruction of a non-binary block code from an intercepted sequence with application to Reed-Solomon codes, IEICE Trans. Fundam. Electron. Commun. Comput. Sci. E95-A (11) (Nov. 2012) 1873–1880, https://doi.org/10.1587/transfun.E95.A.1873.

[15] G. Sicot, S. Houcke, Blind detection of interleaver parameters, Signal Process. 89 (4) (2009) 450–462, https://doi.org/10.1016/j.sigpro.2008.09.012.

[16] R. Swaminathan, A.S. Madhukumar, G. Wang, T.S. Kee, Blind reconstruction of Reed-Solomon encoder and interleavers over noisy environment, IEEE Trans. Broadcast. 64 (4) (Dec. 2018) 830–845, https://doi.org/10.1109/TBC.2018.2795461.

[17] Y.G. Debessu, H.-C. Wu, H. Jiang, Novel blind encoder parameter estimation for turbo codes, IEEE Commun. Lett. 16 (12) (Dec. 2012) 1917–1920, https://doi.org/10.1109/LCOMM.2012.102612.121473.

[18] P. Yu, J. Li, H. Peng, A least square method for parameter estimation of rsc subcodes of turbo codes, IEEE Commun. Lett. 18 (4) (Apr. 2014) 644–647, https://doi.org/10.1109/LCOMM.2014.022514.140086.

[19] J.-P. Tillich, A. Tixier, N. Sendrier, Recovering the interleaver of an unknown turbo-code, in: Proc. IEEE ISIT, 2014, pp. 2784–2788.

[20] M. Teimouri, A. Hedayat, Parameter estimation of turbo code encoder, Adv. Electr. Eng. 282108 (Aug. 2014) 1–6, https://doi.org/10.1155/2014/282108.

[21] R. Swaminathan, A.S. Madhukumar, N.W. Teck, S.C.M. Samson, Parameter estimation of block and helical scan interleavers in the presence of bit errors, Digit. Signal Process. 60 (Jan. 2017) 20–32, https://doi.org/10.1016/j.dsp.2016.08.006.

[22] L. Lu, K.H. Li, Y.L. Guan, Blind detection of interleaver parameters for non-binary coded data streams, in: Proc. IEEE International Conference on Communications (ICC), 2009, pp. 1–4.

[23] L. Lu, K.H. Li, Y.L. Guan, Blind identification of convolutional interleaver parameters, in: Proc. IEEE International Conference on Information, Communications and Signal Processing (ICICS), 2009, pp. 1–4.

[24] R. Swaminathan, A.S. Madhukumar, N.W. Teck, S.C.M. Samson, Parameter estimation of convolutional and helical interleavers in a noisy environment, IEEE Access 5 (2017) 6151–6167, https://doi.org/10.1109/ACCESS.2017.2684189.

[25] Y.-Q. Jia, L.-P. Li, Y.-Z. Li, L. Gan, Blind estimation of convolutional interleaver parameters, in: Proc. IEEE International Conference on Wireless Communications, Networking and Mobile Computing (WiCOM), 2012, pp. 1–4.

[26] C. Choi, D. Yoon, Novel blind interleaver parameter estimation in a non-cooperative context, IEEE Trans. Aerosp. Electron. Syst. 55 (4) (Aug. 2019) 2079–2085, https://doi.org/10.1109/TAES.2018.2875570.

[27] S. Lin, D.J. Costello, Error Control Coding, 2nd ed., Pearson Educ., Upper Saddle River, NJ, USA, 2004.

Swaminathan R is currently working as an Assistant Professor in the Discipline of Electrical Engineering, IIT Indore, after working as a Postdoctoral Research Fellow in the School of Computer Science and Engineering, Nanyang Technological University (NTU) Singapore from 2016 to 2019. Earlier, he completed his PhD from IIT Kharagpur in 2016. He received the B.Tech. degree in ECE from SASTRA University, Thanjavur, in 2009 and M.E. degree in communication systems from the College of Engineering Guindy, Anna University, Chennai, in 2011. His current research focus is on designing hybrid free space optics/radio frequency communication systems for next-generation terrestrial and satellite communication, proposing algorithms for blind parameter estimation of forward error correcting codes and interleavers considering non-cooperative scenarios and validating the same using real data obtained from hardware testbed. In addition, his research interests include but not limited to Index modulation techniques for next-generation wireless communication, Simultaneous Lightwave Information and Power Transfter (SLIPT), Non-Orthogonal Multiple Access (NOMA) techniques, Automatic channel code and interleaver identification techniques, etc. He received the gold medal from the College of Engineering Guindy, Anna University. Furthermore, he has been serving as a Reviewer for reputed IEEE journals and as a TPC member for reputed IEEE conferences.

A.S. Madhukumar's expertise lies in the areas of multi-tier cellular architecture, cooperative and cognitive radio systems, interference management, coding and modulation, new multiple access schemes, hybrid radio systems and other advanced signal processing algorithms for future communication systems. He is involved in a number of funded research projects, organizing international conferences, and a permanent reviewer for many internationally reputed journals and conferences. He has published over 275 referred international conference and journal papers. He is a recipient of Nanyang Award for Teaching Excellence in 2007 and obtained best paper awards in IEEE 35th Digital Avionics Conference in 2016

and in IEEE Integrated Communications, Navigations and Surveillance Conference in 2016 and in 2017. A.S. Madhukumar received his B.Tech degree from College of Engineering, Trivandrum, India, M.Tech from Cochin University of Science and Technology, India and PhD from Department of Computer Science and Engineering, Indian Institute of Technology, Madras, India. He is currently an Associate Professor in the School of Computer Engineering, Nanyang Technological University, Singapore. Before joining NTU, he was involved in communications and signal processing research at Centre for Development of Advanced Computing (Electronics Research and Development Centre), Govt. of India and Institute for Infocomm Research (Centre for Wireless Communications), Singapore. Dr. Madhukumar is a senior member of IEEE.